Sensitive quantitative and rapid immunochromatographic diagnosis of clinical samples by scanning electron microscopy - preparing for future outbreaks

Running title: Immunochromatographic diagnosis of disease by SEM

Hideya Kawasaki*[a], Hiromi Suzuki[a], Masato Maekawa[b], Takahiko Hariyama*[a]

[a] Institute for NanoSuit Research, Preeminent Medical Photonics Education & Research Center, Hamamatsu University School of Medicine, Hamamatsu, Japan

[b] Department of Laboratory Medicine, Hamamatsu University School of Medicine, Hamamatsu, Japan

* Corresponding authors: Hideya Kawasaki, Takahiko Hariyama

Email: gloria@hama-med.ac.jp, hariyama@hama-med.ac.jp

ORCID account: 0000-0001-8923-7722, 0000-0001-9623-1011

Author Contributions: H.K. designed research; H.K., H.S., performed research; H.K. M.M., analyzed data; and H.K., T.H. wrote the paper.

Abbreviations: EM, Electron microscopy; LAMP, loop-mediated isothermal amplification; SEM, scanning electron microscope; GNP, gold nanoparticles; INSM, immunochromatography-NanoSuit® method; PCR, polymerase chain reaction; rRT-PCR, real-time reverse transcription-polymerase chain reaction, IgG, immunoglobulin G; IgM, immunoglobulin M

Abstract

Background: As pathogens such as influenza virus and severe acute respiratory syndrome coronavirus 2 (SARS-CoV-2) can easily cause pandemics, rapid diagnostic tests are crucial for implementing efficient quarantine measures, providing effective treatments to patients, and preventing or containing a pandemic infection. Here, we developed the immunochromatography-NanoSuit® method, an improved immunochromatography method combined with a conventional scanning electron microscope (SEM), which enables observation of immunocomplexes labeled with a colloidal metal.

Methods and Findings: The detection ability of our method is comparable to that of real-time reverse transcription-polymerase chain reaction and the detection time is approximately 15 min. Our new immunochromatography-NanoSuit® method

suppresses cellulose deformity and makes it possible to easily focus and acquire high-resolution images of gold/platinum labeled immunocomplexes of viruses such as influenza A, without the need for conductive treatment as with conventional SEM. Electron microscopy (EM)-based diagnosis of influenza A exhibited 94% clinical sensitivity (29/31) (95% confidence interval [95%CI]: 78.58–99.21%) and 100% clinical specificity (95%CI: 97.80–100%). EM-based diagnosis was significantly more sensitive (71.2%) than macroscopic diagnosis (14.3%), especially in the lower influenza A-RNA copy number group. The detection ability of our method is comparable to that of real-time reverse transcription-polymerase chain reaction.

Conclusions: This simple and highly sensitive quantitative analysis method involving immunochromatography can be utilized to diagnose various infections in humans and livestock, including highly infectious diseases such as COVID-19.

Introduction

Infections are major threats to humanity. The novel influenza A (H1N1) pdm09 was declared a pandemic in 2009 [1], and the current 2020 severe acute respiratory syndrome coronavirus 2 (SARS-CoV-2) pandemic has had a devastating impact on human health and the world economy. The following factors are crucial for

57 reducing the effects of these infections: 1: delayed invasion of infection into the
58 country because of border measures and quarantine, 2: early containment
59 strategies, 3: early diagnosis enabling appropriate treatment, and 4:
60 broad antibody (IgM, IgG) and/or antigen testing against the virus to assess the
61 spread of the virus. Therefore, rapid diagnostic tests are crucial for disease
62 prevention, treatment, and pandemic containment [2]. Although real-time reverse
63 transcription-polymerase chain reaction (rRT-PCR) is a sensitive method, it is time-
64 consuming, costly, and requires special equipment with professional expertise and
65 high-quality samples. For point-of-care testing, immunochromatography is easier
66 to perform and useful for prompt disease detection, but its sensitivity and specificity
67 are lower than those of rRT-PCR. However, improved specificity has been
68 achieved by using lateral flow biosensors (LFBs) with micro- and nano-materials
69 [3]. Signal readouts based on color, electrochemical signals, magnetic properties,
70 luminescent, and surface-enhanced Raman spectroscopy have been integrated
71 with LFBs for quantification analyses [3,4]. Nevertheless, these nanoparticle
72 sensing methods are indirect. Direct observation of metal nanoparticles by electron
73 microscopy (EM) for clinical use has not been reported because of the complexity
74 of sample preparation and conventional EM operation. We recently reported a
75 method for evaluating multicellular organisms in high vacuum of an EM by
76 encasing them in a thin, vacuum-proof suit, the 'NanoSuit®' [5], which can impart

77 conductivity to a wet sample to avoid electron charges. Here, we combined the
78 NanoSuit® method with immunochromatography. The new
79 immunochromatography-NanoSuit® method (INSM) suppresses the deformity of
80 the immunochromatography substrate such as cellulose, which causes blurring of
81 particle images, and enables easy focus and acquisition of high-resolution images
82 without the need for additional conductive treatment [6] as with a conventional
83 scanning EM (SEM). In the medical field, using rRT-PCR and INSM as two
84 sensitive rapid diagnostic tests will help maintain patient health. INSM also is a
85 highly sensitive diagnostic tool for several pathogenic infections or other diagnoses.
86

87 ## Methods

88 ### Ethical statement

89 The study was approved by the Hamamatsu University School of Medicine ethical
90 committee (No. 19-134), and all methods were performed following relevant
91 guidelines and regulations.

92 ### Immunochromatography kit

93 The ImunoAce® Flu kit (NP antigen detection), a human influenza commercial
94 diagnosis kit, was purchased from TAUNS Laboratories, Inc. (Shizuoka, Japan).

95 Au/Pt nanoparticles were utilized to visualize the positive lines. A total of 197
96 clinical samples from patients suspected to be suffering from influenza were
97 provided by a general hospital at the Hamamatsu University School of Medicine
98 for examination using the Flu kit. After macroscopic diagnosis using the Flu kit, the
99 samples were stored in a biosafety box at room temperature (20-25 °C / 68 - 77 °F).
100 The IgM detection immunochromatography kit against SARS-CoV-2 was obtained
101 from Kurabo Industries, Ltd. (Osaka, Japan).

102 **One step rRT-PCR for influenza A**

103 rRT-PCR for influenza A was performed as described previously using Flu A
104 universal primers [7]. A Ct within 38.0 was considered as positive according to the
105 CDC protocol [8]. The primer/probe set targeted the human RNase P gene and
106 served as an internal control for human nucleic acid as described previously [9].

107 **SEM image acquisition**

108 The immunochromatography kit was covered with modified NanoSuit® solution
109 based on previously published components [5] (Nisshin EM Co., Ltd., Tokyo,
110 Japan), placed first onto the wide stage of the specimen holder, and then placed

111 in an Lv-SEM (TM4000Plus, Hitachi High-Technologies, Tokyo, Japan). Images
112 were acquired using backscattered electron detectors with 10 or 15 kV at 30 Pa.

113 **Particle counting**

114 In fields containing fewer than 50 particles/field, the particles were counted
115 manually. Otherwise, ImageJ/Fiji software was used for counting. ImageJ/Fiji uses
116 comprehensive particle analysis algorithms that effectively count various particles.
117 Images were then processed and counting was performed according to the
118 protocol [10].

119 **Diagnosis and statistics**

120 The EM diagnosis and criteria for a positive test were defined as follows: particle
121 numbers from 6 fields from the background area and test-line were statistically
122 analyzed using the *t*-test. If there were more than 5 particles in one visual field and
123 a significant difference ($P < 0.01$) was indicated by the *t*-test, the result was
124 considered as positive. Statistical analysis using the *t*-test was performed in Excel
125 software. Statistical analysis of the assay sensitivity and specificity with a 95%
126 confidence interval (95% CI) was performed using the MedCalc statistical website.
127 The approximate line, correlation coefficient, and null hypothesis were calculated
128 with Excel software.

129

130 ## Results

131 To investigate the sensitivity and specificity of immunochromatography using the
132 NanoSuit® method, an influenza diagnostic kit (TAUNS Laboratories, Inc.) was
133 prepared (**Fig. 1*A***). Two specific antibodies were used: one (anti-mouse IgG or
134 anti-influenza A NP) was immobilized on chromatographic paper, whereas the
135 other was labeled with colloidal gold/platinum (100−200 nm in diameter) and
136 infiltrated into the sample pad. The kit was completed by attaching the sample pad
137 at the end of the membrane. When the clinical sample in lysis buffer (150 □L) was
138 placed on the sample pad, the virus antigen in the sample formed an
139 immunocomplex with the colloidal gold/platinum- labeled antibody, which
140 subsequently formed an immune complex with the antibody immobilized on the
141 membrane, resulting in the generation of colored lines and indicating the presence
142 of the antigen of interest in the sample (**Fig. 1*B* top, middle**). After the reaction,
143 NanoSuit® solution (100 μL) was added upstream of the test-line (**Fig. 1*B* middle**),
144 forming a thin NanoSuit® liquid layer (pale blue) (**Fig. 1*B* bottom**). The kit was
145 positioned on the sample stage in the sample chamber of the SEM as close and
146 parallel as possible to the camera (**Fig. 1*C***). The observation position of the test-
147 line and background area were determined at fixed distances from the control-line

148 border. The number of Au/Pt particles at the test-line and background area were
149 counted in 6 fields of view at ×1200 (**Fig. 1*D***). Without NanoSuit® treatment,
150 swelling of the cellulose and residual liquid present due to electron beam energy
151 were observed (**Fig. 2*A***). In contrast, following NanoSuit® treatment, the cellulose
152 membrane showed little or no swelling (**Fig. *2B***).

153 The SEM images of the test lines and background were compared. **Figure 3*A,***
154 ***D*** show the "macroscopic diagnosis-positive" test-line. **Figure 3*B, E*** are images of
155 the "macroscopic diagnosis-negative" and "EM diagnosis-positive" test-line.
156 **Figure 3*C***, ***F*** are the images of the background. Au/Pt particles (arrows) of the
157 test-line were clearly visualized (**Fig. 3*A, B, D, E***) compared to background areas
158 of the cellulose membrane (**Fig. 3*C, F***). Au/Pt particle counting was performed by
159 using ImageJ/Fiji software for macroscopic diagnosis-positive samples. Manual
160 counting was performed for the images of "background" and "macroscopic
161 diagnosis negative and SEM diagnosis-positive" samples as well as "EM-negative"
162 samples. Another immunochromatography diagnosis kit for detecting IgM
163 antibodies against SARS-CoV-2 from Kurabo Industries, Ltd. was tested using the
164 NanoSuit® method (**S1*A* Fig**). The cellulose membrane image without the
165 immunocomplex was clearly visualized after NanoSuit® treatment (**S1*B* Fig**).

166 Approximately 25-nm countable gold nanoparticles (GNPs) of the control-line were
167 detected (**S1*C* Fig).**

168 Diagnoses based on macroscopic, EM, and rRT-PCR results were compared
169 using the 197 influenza-suspected clinical samples. rRT-PCR for influenza A was
170 performed with the same clinical pharyngeal swab samples as used in
171 immunochromatography. To examine the relationship between the influenza copy
172 number and rRT-PCR threshold, serial dilutions were prepared (**S2*A* Fig**). A
173 calibration curve (**S2*B* Fig**) was drawn to determine the relationship between the
174 copy number and cycle threshold (Ct) (**S2*C* Fig**). In our assay system, Ct ≤ 38.0
175 was calculated to be ≥ 151.4 copies/reaction.

176 The quantitative relationship between particle counts/fields (log10) and Ct are
177 shown as a scatter diagram. The correlation coefficient of Ct and particle
178 counts/field was -0.803, which was significant (p = 3.79E-08) and the null
179 hypothesis was rejected (**Fig. 4**) (**Supplemental data**).

180 The EM diagnosis for influenza A showed 94% clinical sensitivity (29/31) (95%
181 confidence interval [95%CI]: 78.58–99.21%) and 100% clinical specificity (95%CI:
182 97.80–100%) (**Table 1**) (**Supplemental data**), as well as a strong correlation
183 (kappa; 0.99) compared with the results obtained by rRT-PCR (14.0 ≤ Ct ≤ 38.0)
184 (**Table 2**) (**Supplemental data**). In contrast, standard macroscopic diagnosis

185 showed 77% clinical sensitivity (24/31) (95%CI: 58.90–90.41%) and 100% clinical
186 specificity (95%CI: 97.80–100%) (**Table 1**) (**Supplemental data**), along with a
187 strong correlation (kappa; 0.96) compared with the results obtained by rRT-PCR
188 (14.0 ≤ Ct ≤ 38.0) (**Table 2**)(**Supplemental data**).

189

190 Discussion

191 Rapid diagnostic tests show variable assay performance with sensitivities of 10–
192 70% and up to 90% specificity compared to standard rRT-PCR-based assays [11].
193 Their sensitivity has been improved by employing europium nanoparticles, which
194 show 82.59% sensitivity and 100% specificity for clinically evaluated influenza A
195 (H1N1) [12]. The use of silver amplification immunochromatography in influenza
196 virus detection kits showed 91.2% sensitivity and 95.8% specificity [13]. Moreover,
197 the rapid fluorescent immunochromatographic test employing CdSe/CdS/ZnS
198 quantum dots showed 93.75% clinical sensitivity and 100% clinical specificity [14].
199 However, the potential toxic effects of cadmium-based quantum dots are
200 controversial [15]. INSM is safe and showed the highest sensitivities (94% clinical
201 sensitivity, 100% clinical specificity) in this study. Generally, overall sensitivity
202 depends on the distribution of each sample's pathogen-copy number in the
203 investigated group. Our study revealed that EM diagnosis was significantly more

204 sensitive (71.2%) than macroscopic diagnosis (14.3%) in the lower copy number
205 group (30.0 ≤ Ct ≤ 38). The detection ability of our method is comparable to that of
206 rRT-PCR (**Fig. 4**). Theoretically and practically, our method shows the highest
207 detection performance as an immunochromatographic diagnostic method. More
208 sensitive immunochromatographic products may be developed in future through
209 further improvements such as by optimizing the antigen concentration.

210 PCR has recently been used as a main diagnostic tool for SARS-CoV-2. The
211 introduction of immunochromatography analysis using the SARS-CoV-2 antigen
212 has greatly changed testing practices. All immunochromatographic-negative
213 SARS-CoV-2-suspected samples are recommended for analysis by PCR. Highly
214 sensitive immunochromatographic tests for infectious diseases can greatly reduce
215 the number of PCR samples to be analyzed. Furthermore, Cohen and Kessel
216 reported high false-positive rates of RT-PCR testing for SARS-CoV-2 using clinical
217 samples. Overall, 336 of 10,538 negative samples (3.2%) were reported as
218 positive. In contrast, <0.6–7.0% false-positive rates in external quality
219 assessments of RNA virus assays were reported for influenza A. The amplification
220 of nucleic acids makes PCR-based assays highly sensitive but highly vulnerable
221 to minute levels of sample contamination which can produce false-positive results
222 indistinguishable from true-positive results [16]. The same pitfall may be found in
223 Loop-Mediated Isothermal Amplification (LAMP) method. We propose that

224 macroscopic immunochromatographic-negative and PCR- or LAMP-positive
225 cases should be compared with highly sensitive immunochromatographic data
226 such as that obtained by INSM as well as clinical data to reduce false-positive
227 cases.

228 Although ImageJ/Fiji is useful software, it should be further developed to
229 increase its reliability. The development of an automated GNP counting system to
230 replace manual counting using deep learning is being evaluated by our team.
231 Furthermore, clinical application of using an automated inexpensive SEM for
232 immunochromatography in combination with INSM for SEM shows potential.
233 Among the commonly used micro/nano-particles in immunochromatography,
234 colloidal GNP is the most widely used [3]. GNP is safe and can be easily
235 conjugated with biomolecules that retain their biochemical activity upon binding.
236 Therefore, developing new GNP-based LFBs may be easier and faster than
237 developing micro/nano-materials and can be adapted quickly for new emerging
238 infections such as SARS-CoV-2 [17]. Investigation of INSM using smaller GNPs is
239 currently underway. INSM is applicable to all LFBs, particularly in emergency tests
240 to evaluate troponin, brain natriuretic peptide, and procalcitonin as measured by
241 immunochromatography.

242 Diagnosis using the INSM shows high sensitivity, as it allows for direct particle
243 observation. Our results indicate that INSM can be used for automated quantitative
244 measurement in any immunochromatographic tests including recently developed
245 SARS-CoV-2 antigen or IgM/IgG antibodies tests against SARS-CoV-2. This
246 method can be used to promptly diagnose new emerging infections including those
247 in livestock and promote innovations in assays using LFBs.

248

249 **Acknowledgments**

250 The authors thank Noriko Aoki (TAUNS Laboratories, Inc.) for providing rRT-PCR
251 data on influenza A and Takafumi Miwa and Takumi Tandou (Hitachi, Ltd.
252 Research & Development Group Nano-process Research Department) for
253 advising on SEM. We also thank the clinical laboratory center of Hamamatsu
254 University School of Medicine, University Hospital for providing influenza
255 immunochromatography test strips after routine examinations. This work was
256 supported by JST START (grant number 714 [to H.K.]), JSPS KAKENHI (grant
257 numbers JP17K08784 [to H.K.] and JP18H01869 [to T.H.]), and AMED (grant
258 number A508 [to H.K.]).

259

260 **Competing interests**

261 The authors declare no competing interests.

262 ## References

263 [1] Swerdlow DL, Finelli L. Preparation for possible sustained transmission of 2019
264 novel coronavirus: lessons from previous epidemics. JAMA. 2020;323: 1129-1130.
265 [2] Ravina R, Dalal A, Mohan H, Prasad M, Pundir CS. Detection methods for
266 influenza A H1N1 virus with special reference to biosensors: a review. Biosci Rep.
267 2020;40.
268 [3] Huang Y, Xu T, Wang W, Wen Y, Li K, Qian L, et al. Lateral flow biosensors based
269 on the use of micro- and nanomaterials: a review on recent developments.
270 Mikrochim Acta. 2019;187: 70.
271 [4] Urusov AE, Zherdev AV, Dzantiev BB. Towards lateral flow quantitative assays:
272 detection approaches. Biosensors (Basel). 2019;9.
273 [5] Takaku Y, Suzuki H, Ohta I, Ishii D, Muranaka Y, Shimomura M, et al. A thin
274 polymer membrane, nano-suit, enhancing survival across the continuum between
275 air and high vacuum. Proc Natl Acad Sci USA. 2013;110: 7631-7635.
276 [6] Kawasaki H, Itoh T, Takaku Y, Suzuki H, Kosugi I, Meguro S, et al. The NanoSuit
277 method: a novel histological approach for examining paraffin sections in a
278 nondestructive manner by correlative light and electron microscopy. Lab Invest
279 2020;100: 161-173.
280 [7] de-Paris F, Beck C, Machado ABMP, Paiva RM, da Silva Menezes D, de Souza
281 Nunes L, et al. Optimization of one-step duplex real-time RT-PCR for detection of

282 influenza and respiratory syncytial virus in nasopharyngeal aspirates. J Virol
283 Methods. 2012;186: 189-192.
284 [8] CDC. Division CDC Human Influenza Virus Real-Time RT-PCR Diagnostic Panel
285 (CDC Flu rRT-PCR Dx Panel). 2014. Available from:
286 https://journals.plos.org/plosone/article/file?type=supplementary&id=info:doi/10.1
287 371/journal.pone.0201248.s007.
288 [9] WHO Collaborating Centre for Influenza, GA. CDC protocol of realtime RTPCR for
289 influenza A (H1N1) 2009. Available from:
290 https://www.who.int/csr/resources/publications/swineflu/realtimeptpcr/en/.
291 [10] O'Brien J, Hayder H, Peng C. Automated quantification and analysis of cell
292 counting procedures using ImageJ plugins. J Vis Exp. 2016;17: 54719.
293 [11] Vemula SV, Zhao J, Liu J, Wang X, Biswas S, Hewlett I. Current approaches for
294 diagnosis of influenza virus infections in humans. Viruses. 2016;8: 96.
295 [12] Yu ST, Bui CT, Kim DTH, Ngyuen AVT, Trinh TTT, Yeo SJ. Clinical evaluation of
296 rapid fluorescent diagnostic immunochromatographic test for influenza A virus
297 (H1N1). Sci Rep. 2018;8: 13468.
298 [13] Mitamura K, Zhimizu H, Yamazaki M, Ichikawa M, Nagai K, Katada J, et al. Clinical
299 evaluation of highly sensitive silver amplification immunochromatography systems
300 for rapid diagnosis of influenza. J Virol Methods. 2013;194: 123-128.

301 [14] Nguyen AVT, Dao TD, Trinh TTT, Choi DY, Yu ST, Park H, et al. Sensitive
302 detection of influenza a virus based on a CdSe/CdS/ZnS quantum dot-linked rapid
303 fluorescent immunochromatographic test. Biosens Bioelectron. 2020;155: 112090.
304 [15] Oh E, Liu R, Nel A, Gemill KB, Bilal M, Cohen Y, et al. Meta-analysis of cellular
305 toxicity for cadmium-containing quantum dots. Nat Nanotechnol. 2016;11: 479-486.
306 [16] Cohen AN, Kessel B. False positives in reverse transcription PCR testing for
307 SARS-CoV-2. medRxiv. 2020.
308 [17] Sheridan C. Fast, portable tests come online to curb coronavirus pandemic. Nat
309 Biotechnol. 2020;38: 515-518.

310 **Figures**

311

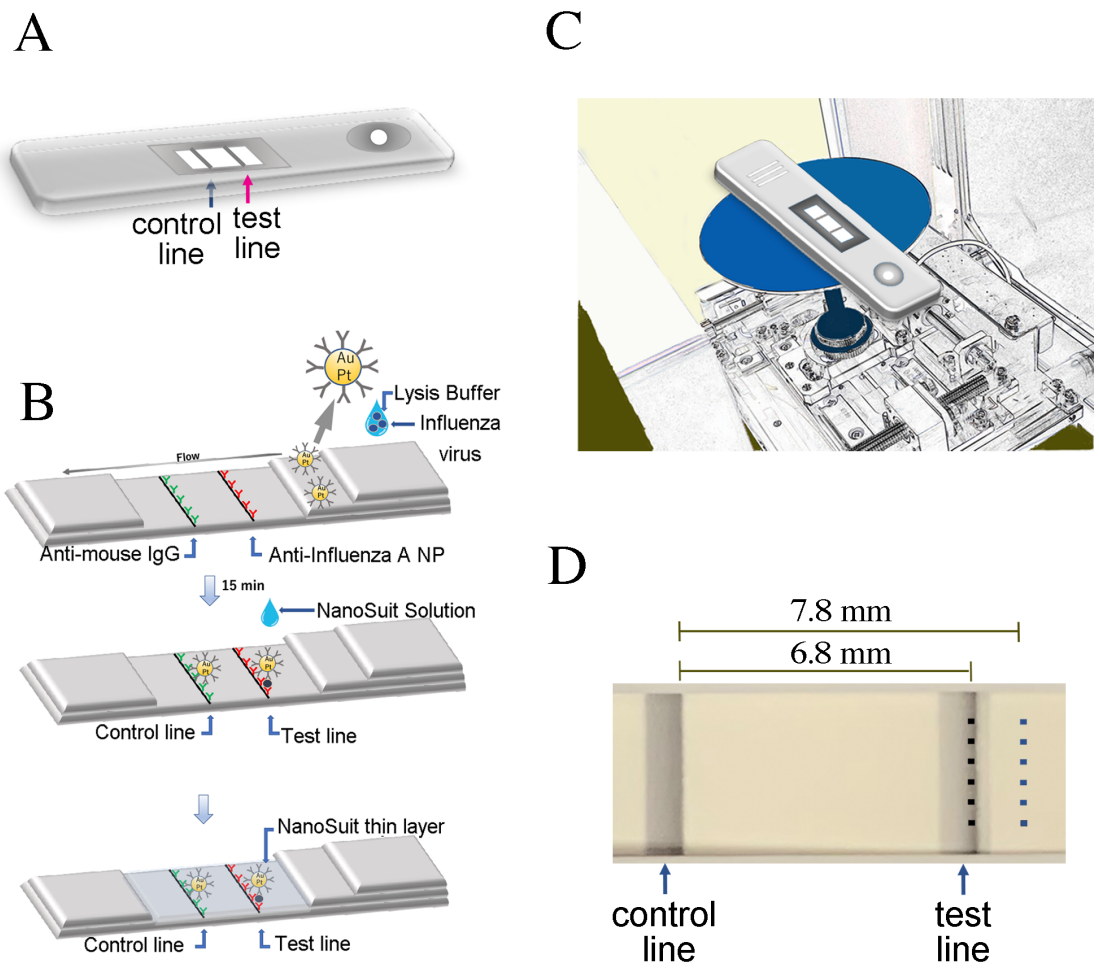

312

313 **Figure 1.** Sensitivity and specificity of immunochromatography using the

314 NanoSuit® method. (***A***) Kit representation showing test and control lines. (***B***)

315 Schematic diagram of the gold/platinum (Au/Pt)-Ab conjugate-linked rapid

316 immunochromatographic kit. The immune-complex reacted with the anti-influenza

317 A nucleoprotein (NP) at the test line and anti-mouse IgG at the control-line (top,

318 middle). A NanoSuit® thin layer was formed after NanoSuit® treatment (bottom).

319 (***C***) Kit placement in the SEM chamber. (***D***) Determination of the observation

320 positions. Six fields were randomly selected in the test line and background areas.

321

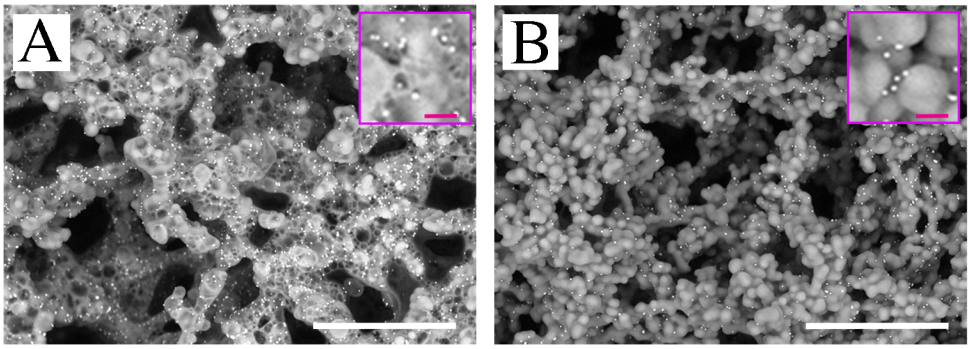

322

323 **Figure 2.** (***A, B***) Images of cellulose and Au/Pt-labeled immunocomplex with

324 immobilized antibody without (***A***) and with NanoSuit treatment (***B***). Scale bars in

325 (***A***) and (***B***) = 15 μm. Inset is magnified image. Scale bars 600 nm.

326

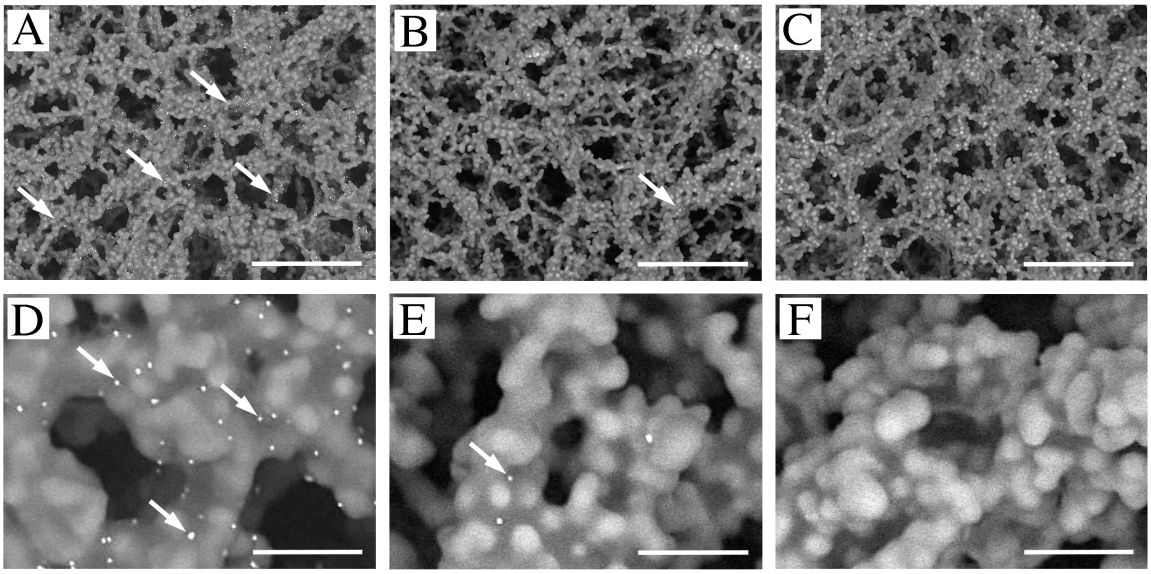

Figure 3. Comparison of SEM images of test lines and of background. (***A, D***) images of "macroscopic diagnosis-positive" test-line. (***B, E)*** Images of "macroscopic diagnosis-negative" and "EM diagnosis-positive" test-line. (***C, F***) Images of "background". White arrows indicate representative Au/Pt particles. Scale bars in (***A, B, C***) = 30 μm and (***D, E, F***) = 3 μm.

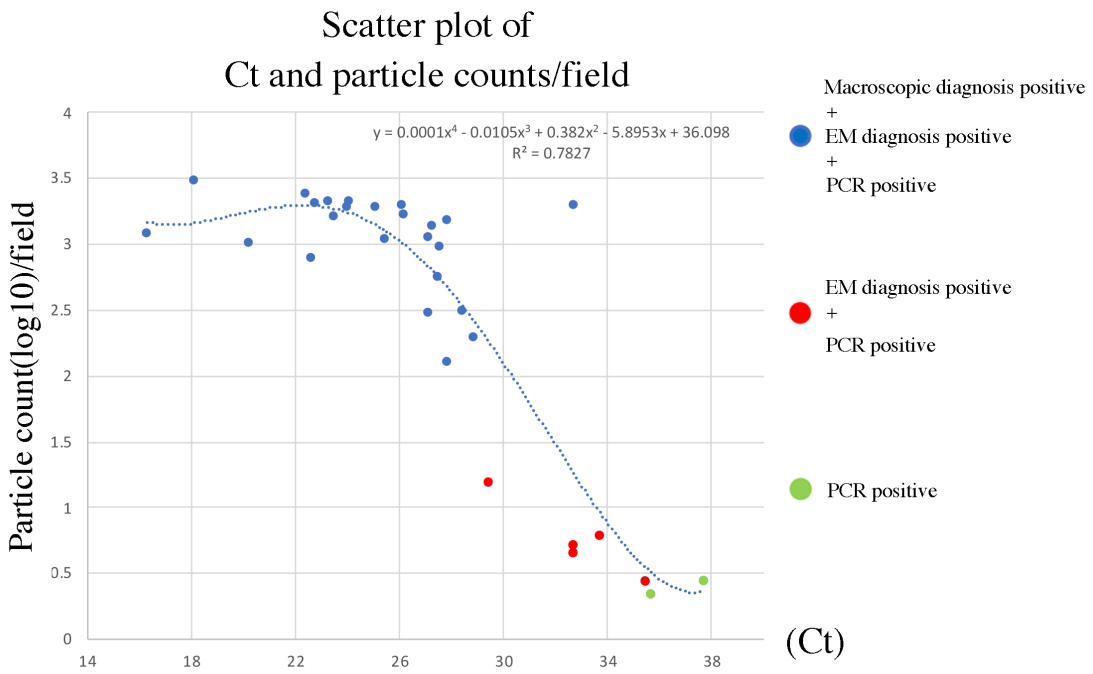

334

335 **Figure 4.** Scatter plot of Ct and particle counts/field. Blue dot represents triple-
336 positive ("macroscopic diagnosis-positive" and "EM diagnosis-positive" and "PCR
337 diagnosis-positive"). Red dot represents double-positive ("EM diagnosis-positive"
338 and "PCR diagnosis-positive"). Green dot represents single-positive ("PCR
339 diagnosis-positive"). Blue dot line is approximate curve. Vertical axis: particle
340 counts (log10)/field. Horizontal axis: Ct of influenza A.

341

342 **Tables**

343

Influenza A rRT-PCR	Ct	Macroscopic diagnosis		Electron microscopic diagnosis	
		Sensitivity	Specificity	Sensitivity	Specificity
Positive (n=31)	14.0≤Ct<22.0	100% (3/3)		100% (3/3)	
	22.0≤Ct<30.0	95.2% (20/21)		100% (21/21)	
	30.0≤Ct≤38.0	14.3% (1/7)		71.4% (5/7)	
	14.0≤Ct≤38.0	77.4% (24/31)		93.5% (29/31)	
Negative (n=166)	Ct>38.0		100% (166/166)		100% (166/166)

Table 1. Clinical diagnostic performance of EM assay. Thirty-one influenza A-rRT-PCR-positive samples were used to determine the sensitivity of the assays, and 166 influenza rRT-PCR-negative samples were used to determine the specificity of the assays.

		Macroscopic diagnosis			Electron microscopic diagnosis		
		positive	negative	Row Marginal	positive	negative	Row Marginal
Influenza A rRT-PCR	Positive	24	7	31	29	2	31
	Negative	0	166	166	0	166	166
Column Marginal		24	172	197	29	168	197
% Agreement(kappa)		0.96: 24+166/197			0.99: 29+166/197		

Table 2. Comparison of EM diagnosis with rRT-PCR and macroscopic diagnosis by immunochromatography.

Supplemental Figures and Data

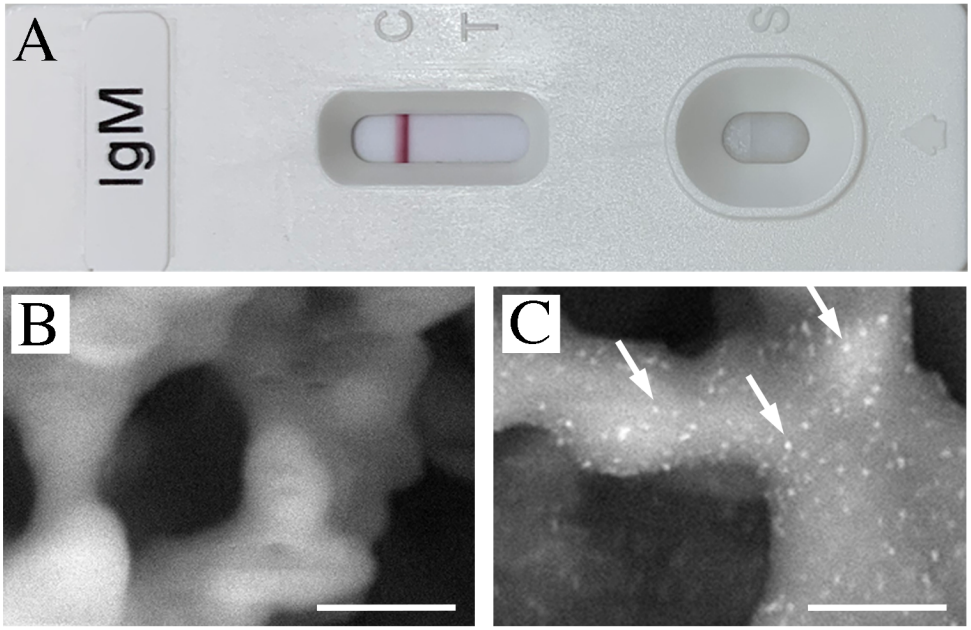

Supplemental Figure 1. (***A***) Immunochromatography diagnosis kit for IgM antibody against SARS-CoV-2. (***B***) Background image. (***C***) Multiple gold

359 nanoparticles (GNPs) (approximately 25-nm diameter) of the control-line on
360 cellulose. White arrows indicate representative GNPs. Scale bars in (***B***) and (***C***) =
361 600 nm.
362

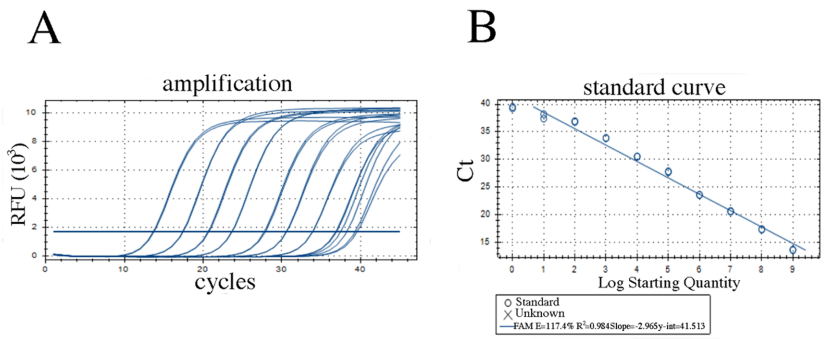

C

Sample (copies/μl)	Flu A Ct	
1.0×10^9	13.62	13.72
1.0×10^8	17.42	17.37
1.0×10^7	20.59	20.69
1.0×10^6	23.64	23.6
1.0×10^5	27.89	27.72
1.0×10^4	30.53	30.57
1.0×10^3	33.9	33.9
1.0×10^2	36.81	36.95
1.0×10^1	37.43	38.22
1.0×10^0	39.27	39.53

Supplemental Figure 2. Comparison of macroscopic, electron microscopic (EM) and rRT-PCR influenza A diagnoses. (***A***) rRT-PCR amplification curve for influenza A. (***B***) Standard curve for rRT-PCR of influenza A. (***C***) Relationship between cycle threshold (Ct) and sample copy numbers/reaction.

Case	Macroscopic Diagnosis	Electron Microscopic Diagnosis	BG: 1 particles/field	BG: 2 particles/field	BG: 3 particles/field	BG: 4 particles/field	BG: 5 particles/field	BG: 6 particles/field	Average BG	TL:1 particles/field	TL:2 particles/field	TL:3 particles/field	TL:4 particles/field	TL:5 particles/field	TL:6 particles/field	Average TL	t-test	Diagnosis	rRT-PCR	CT1	CT2	Average CT	Diagnosis
No. 1	positive		2	2	3	0	1	3	1.83333333	1057	886	1472	1005	1026	1241	1114.5	2.34304E-05	positive		27.13	27.19	27.16	positive
No. 2	positive		9	12	6	7	12	16	10.3333333	1459	2104	1482	759	2424	1292	1586.666667	0.00063971	positive		23.46	23.65	23.51	positive
No. 3	positive		26	17	17	12	11	27	18.3333333	343	362	291	332	259	365	325.3333333	3.06815E-06	positive		28.49	28.46	28.48	positive
No. 4	positive		48	42	24	39	19	20	32	1839	1401	1610	1897	2140	1293	1696.666667	2.67998E-05	positive		26.21	26.21	26.21	positive
No. 5	positive		3	2	0	3	3	4	2.5	332	320	301	291	203	339	297.6666667	1.39772E-05	positive		27.16	27.18	27.17	positive
No. 6	positive		11	7	34	17	27	16	18.6666667	2153	3166	1169	2059	1880	1307	1955.666667	0.000616081	positive		26.12	26.2	26.16	positive
No. 7	positive		15	17	2	15	8	14	11.8333333	987	1334	887	1458	1294	1298	1209.666667	2.04264E-05	positive		16.3	16.37	16.33	positive
No. 8	positive		14	8	5	5	17	18	11.1666667	1162	1570	2462	2013	2375	2404	1997.666667	0.000128189	positive		22.78	22.85	22.82	positive
No. 9	positive		13	31	16	20	8	23	18.5	913	559	811	688	669	1083	787.1666667	9.16168E-05	positive		22.58	22.68	22.63	positive
No.10	positive		21	28	16	16	18	8	17.8333333	972	1037	556	1160	566	1468	959.8333333	0.000644387	positive		27.64	27.59	27.62	positive
No.11	positive		5	5	5	7	4	3	4.83333333	1077	1741	2682	1548	1726	2736	1918.333333	0.000425094	positive		32.7	32.83	32.57	positive
No.12	positive		0	1	0	2	2	6	1.83333333	1682	1984	2295	1973	2081	1417	1905.333333	1.21327E-05	positive		25.1	25.1	25.1	positive
No.13	positive		32	35	15	8	19	12	20.1666667	2981	2579	3371	3044	3232	3090	3049.5	6.83137E-07	positive		18.21	18.15	18.18	positive
No.14	positive		34	36	12	8	12	13	19.1666667	2861	2748	2548	2774	1634	1770	2389.166667	5.91063E-05	positive		22.33	22.49	22.41	positive
No.15	positive		55	22	25	46	60	34	40.3333333	1152	606	490	503	442	399	598.6666667	0.002101821	positive		27.54	27.48	27.51	positive
No.16	positive		42	12	30	27	42	34	31.1666667	1927	988	1100	1162	1339	2577	1515.5	0.000959966	positive		27.85	27.88	27.87	positive
No.17	positive		1	0	3	1	1	2	1.33333333	196	243	171	142	151	244	191.1666667	7.12664E-05	positive		28.99	28.85	28.92	positive
No.18	positive		14	7	4	1	4	4	5.66666667	2207	1756	2748	2085	1766	2087	2108.166667	1.58095E-05	positive		23.33	23.55	23.29	positive
No.19	positive		0	0	2	2	1	3	1.33333333	874	648	993	1153	1280	1055	1000.5	5.17775E-05	positive		20.23	20.29	20.26	positive
No.20	positive		9	1	1	5	11	6	5.5	1776	2260	1765	1605	1866	2106	1896.333333	3.70512E-06	positive		24.1	24.04	24.07	positive
No.21	positive		36	40	37	11	7	4	22.5	2280	2380	2034	2093	2056	1840	2114.166667	4.91638E-07	positive		24.05	24.13	24.09	positive
No.22	positive		2	1	0	1	0	2	1	1163	881	1034	1005	1327	1027	1072.833333	6.28819E-06	positive		25.52	25.51	25.52	positive
No.23	positive		1	0	0	0	0	0	0.16666667	160	187	103	107	92	109	126.3333333	0.000222593	positive		27.85	27.91	27.88	positive
No.24	positive		0	0	0	0	0	1	0.16666667	1156	1487	1377	1403	1448	1308	1363.166667	5.30624E-07	positive		27.24	24.33	27.29	positive
No.25	negative		2	1	1	1	1	3	1.5	6	1	7	8	8	9	6.5	0.003016442	positive		32.76	32.66	32.71	positive
No.26	negative		2	1	0	3	2	1	1.5	18	16	25	20	12	9	16.66666667	0.000789827	positive		29.55	29.5	29.53	positive
No.27	negative		2	0	0	4	0	1	1.16666667	8	5	4	5	5	7	5.666666667	0.001001171	positive		32.73	32.76	32.75	positive
No.28	negative		0	2	2	0	1	1	1	6	5	7	7	11	6	7	0.001112374	positive		33.92	33.56	33.94	positive
No.29	negative		2	4	3	2	1	3	2.5	8	5	3	4	6	5	5.166666667	0.000796697	positive		35.55	35.11	35.65	positive
No.30	negative		15	10	5	8	4	10	8.66666667	12	15	11	9	11	8	10.83333333	0.138669902	negative		35.72	35.77	35.75	positive
No.31	negative		2	0	5	0	0	2	1.5	1	5	2	6	4	7	4.166666667	0.069889516	negative		37.83	37.63	37.73	positive

Supplemental Data. Comparison of among macroscopic diagnosis, EM diagnosis and rRT-PCR diagnosis. BG: Background, TL: Test Line

A

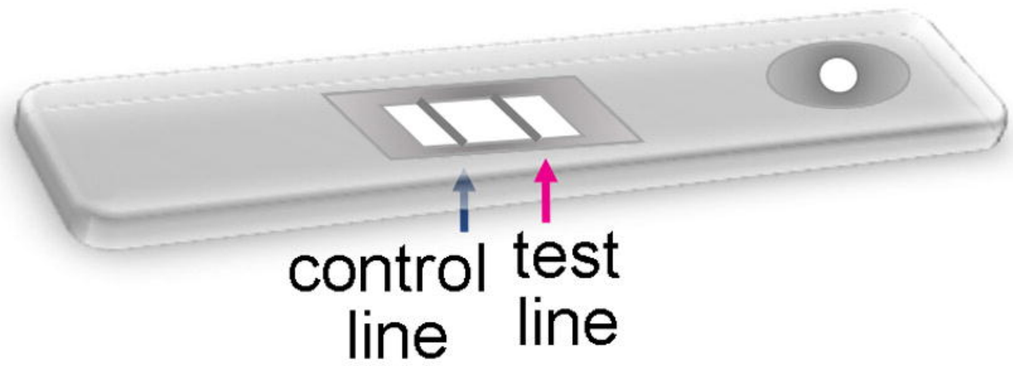
control line
test line

B

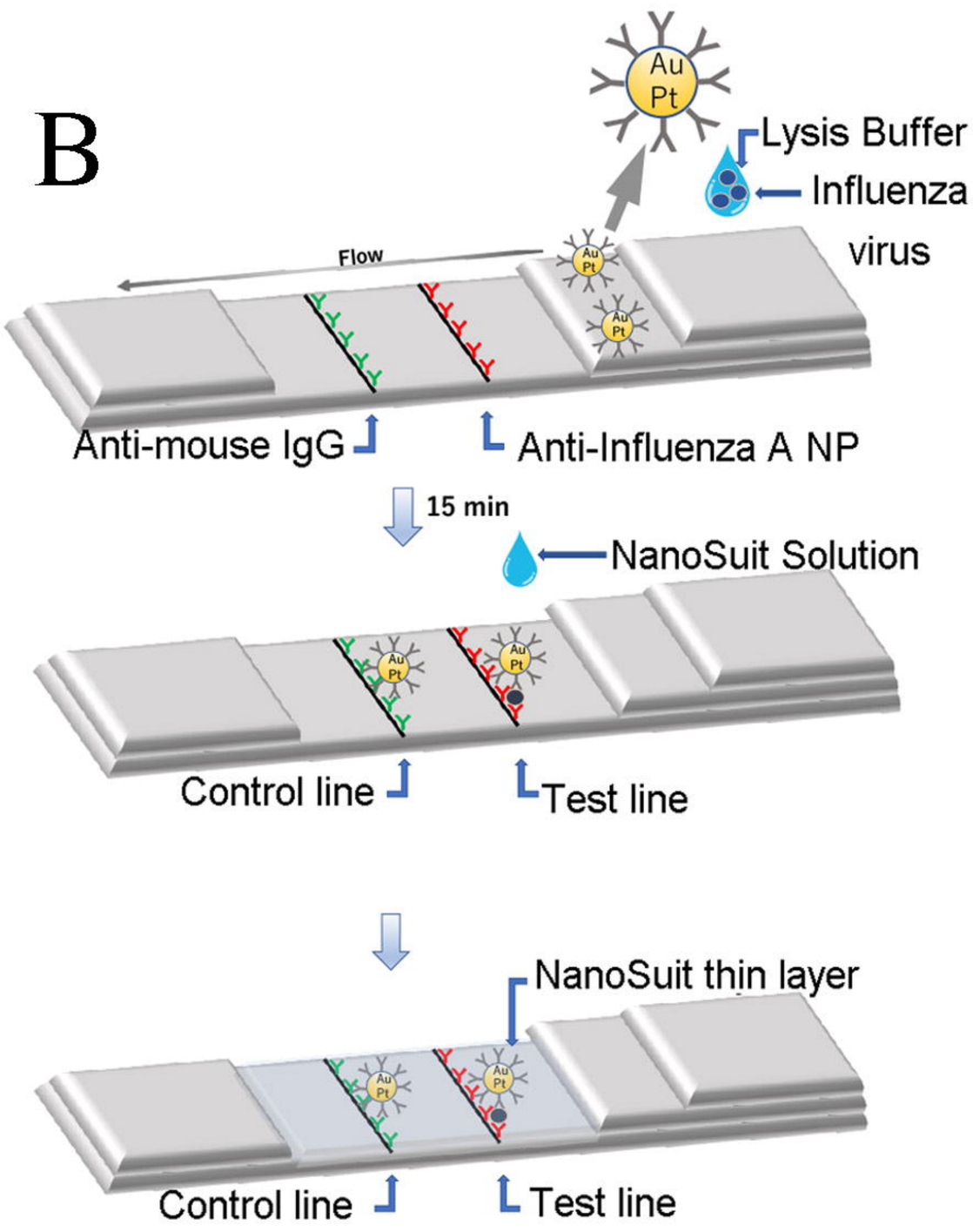
Au Pt
Lysis Buffer
Influenza virus
Flow
Anti-mouse IgG
Anti-Influenza A NP
15 min
NanoSuit Solution
Control line
Test line
NanoSuit thin layer
Control line
Test line

C

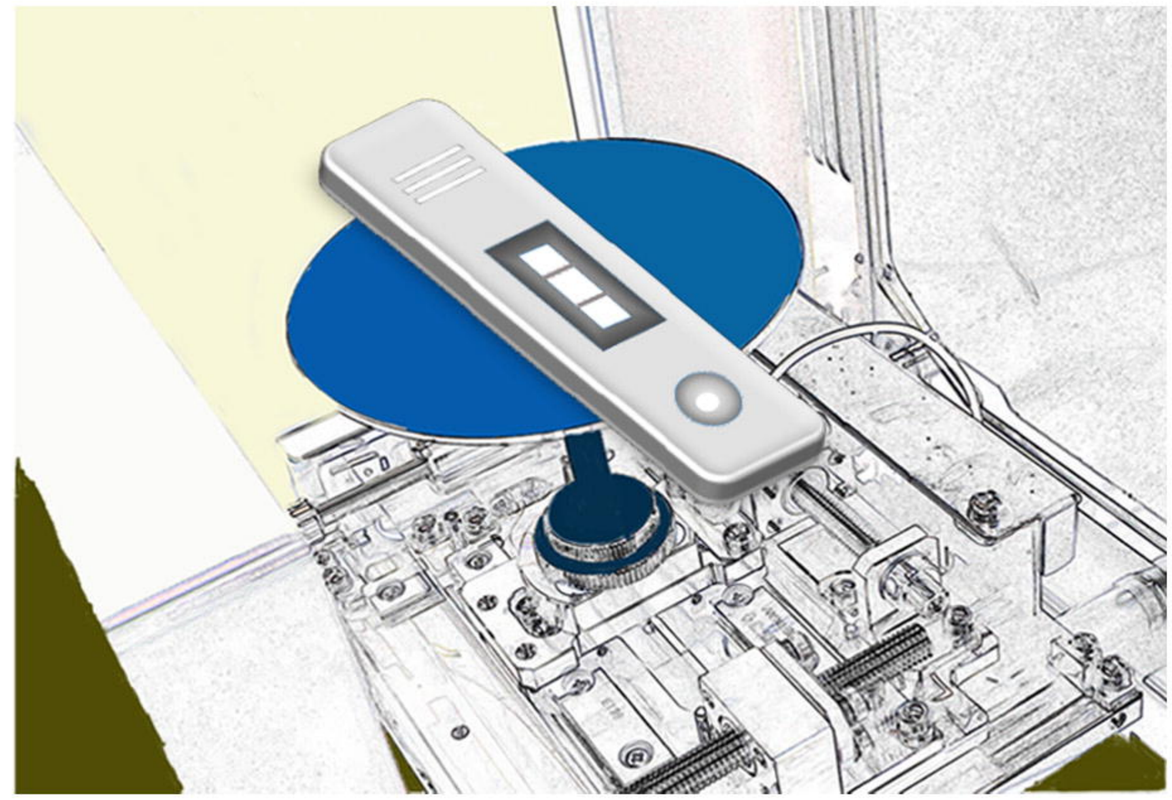

D

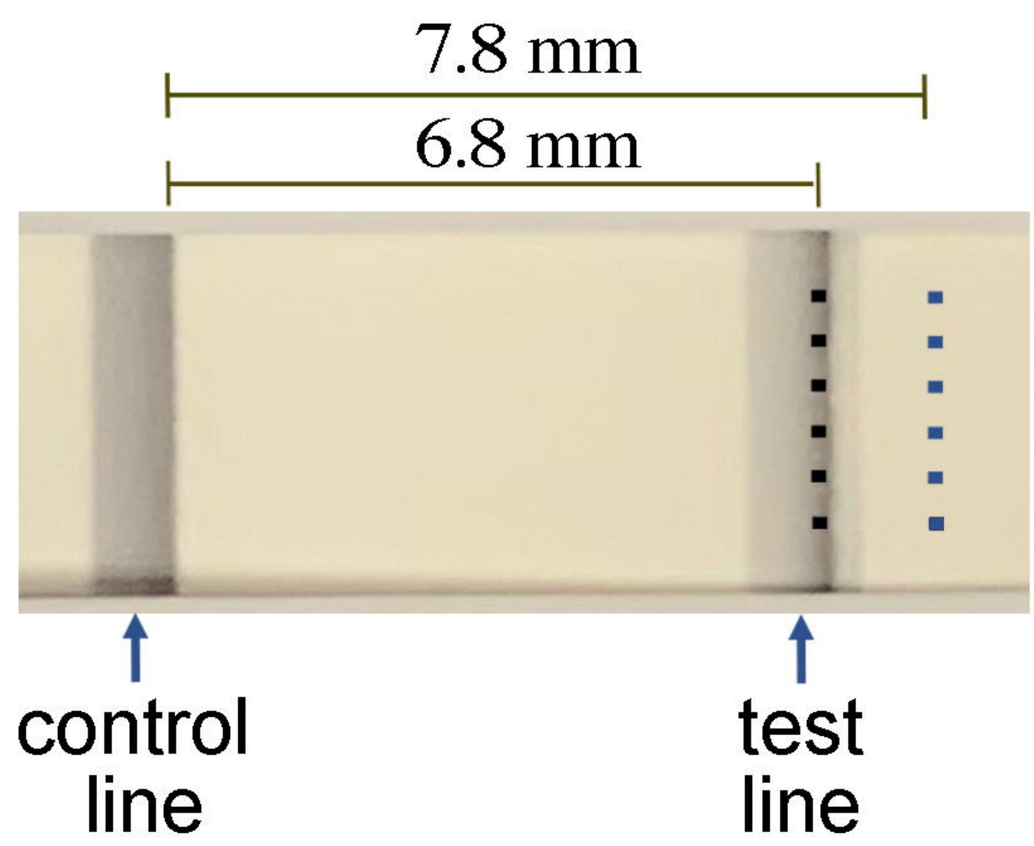
7.8 mm
6.8 mm
control line
test line

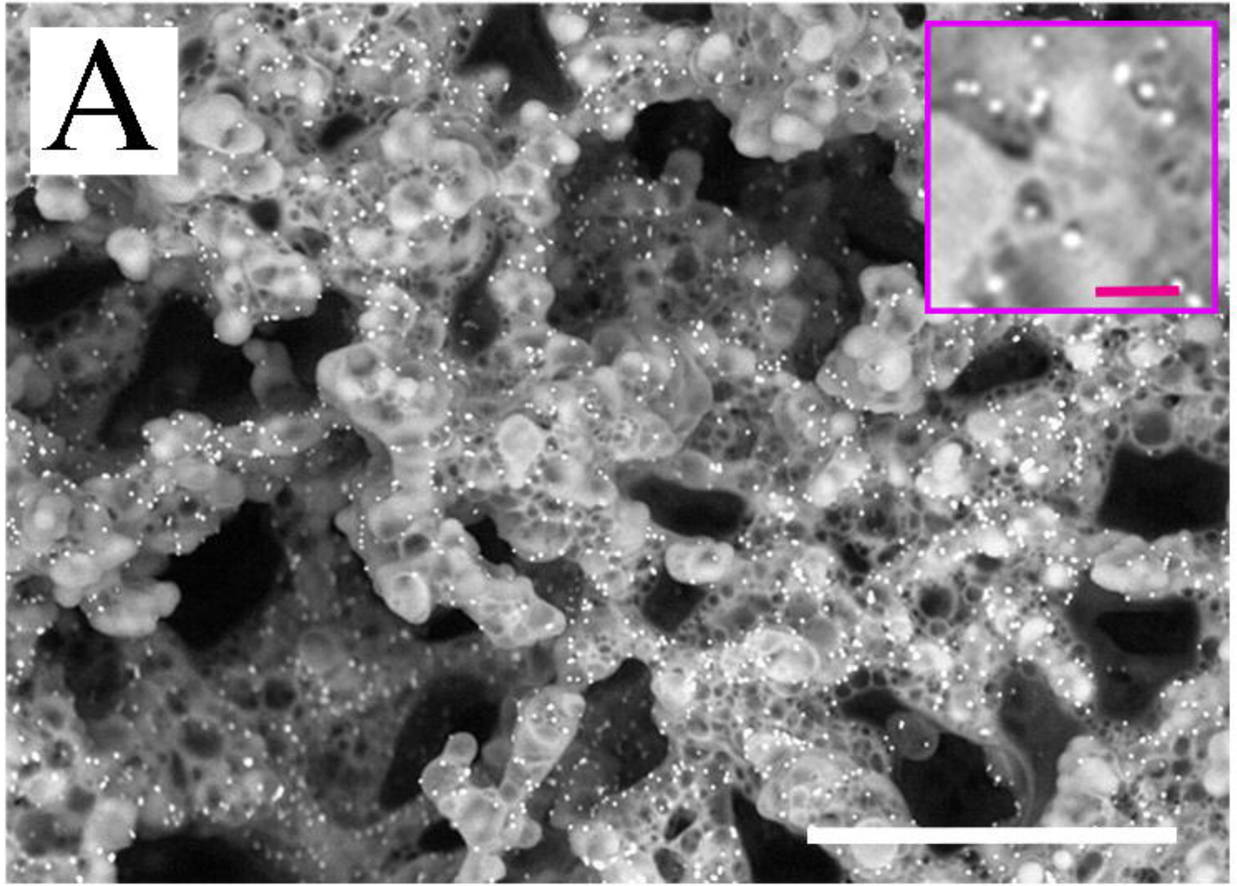
A

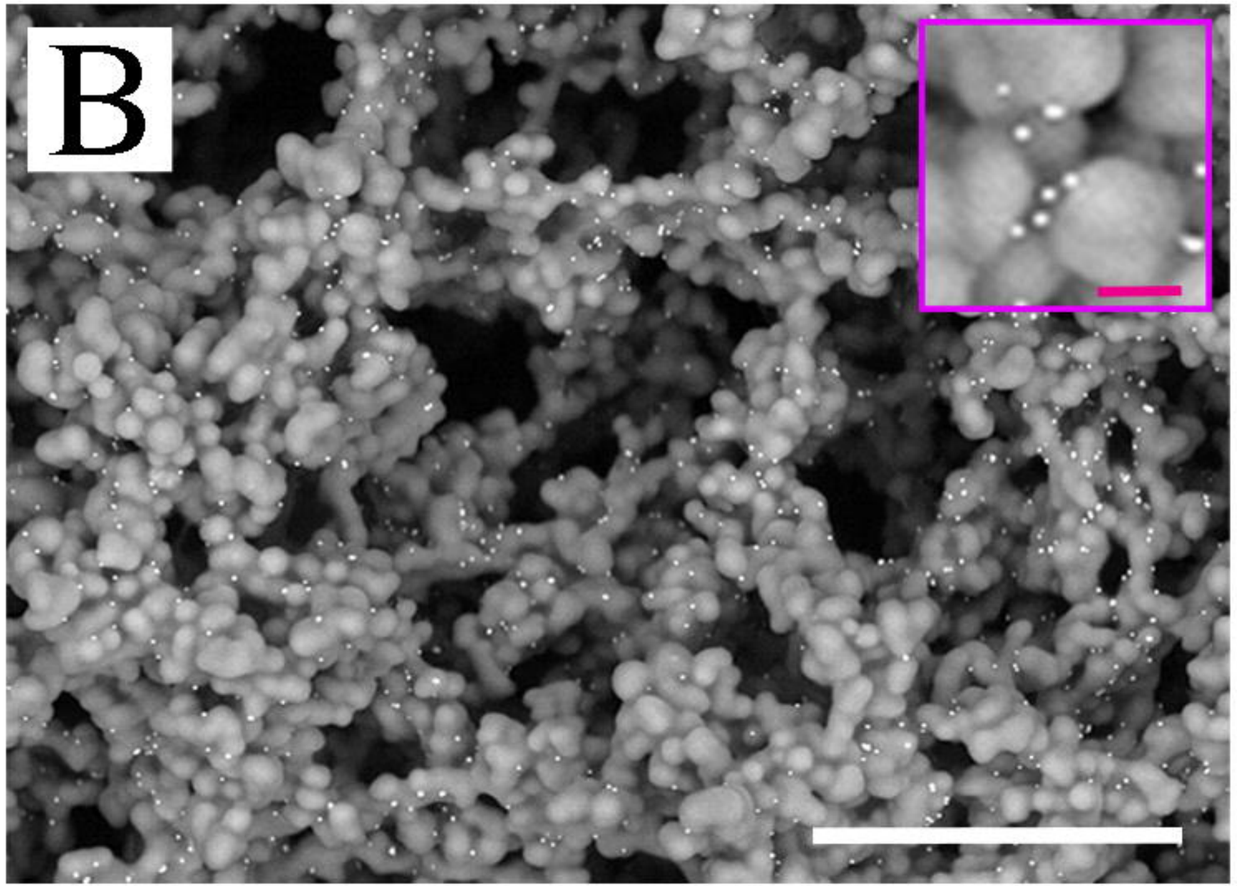
B

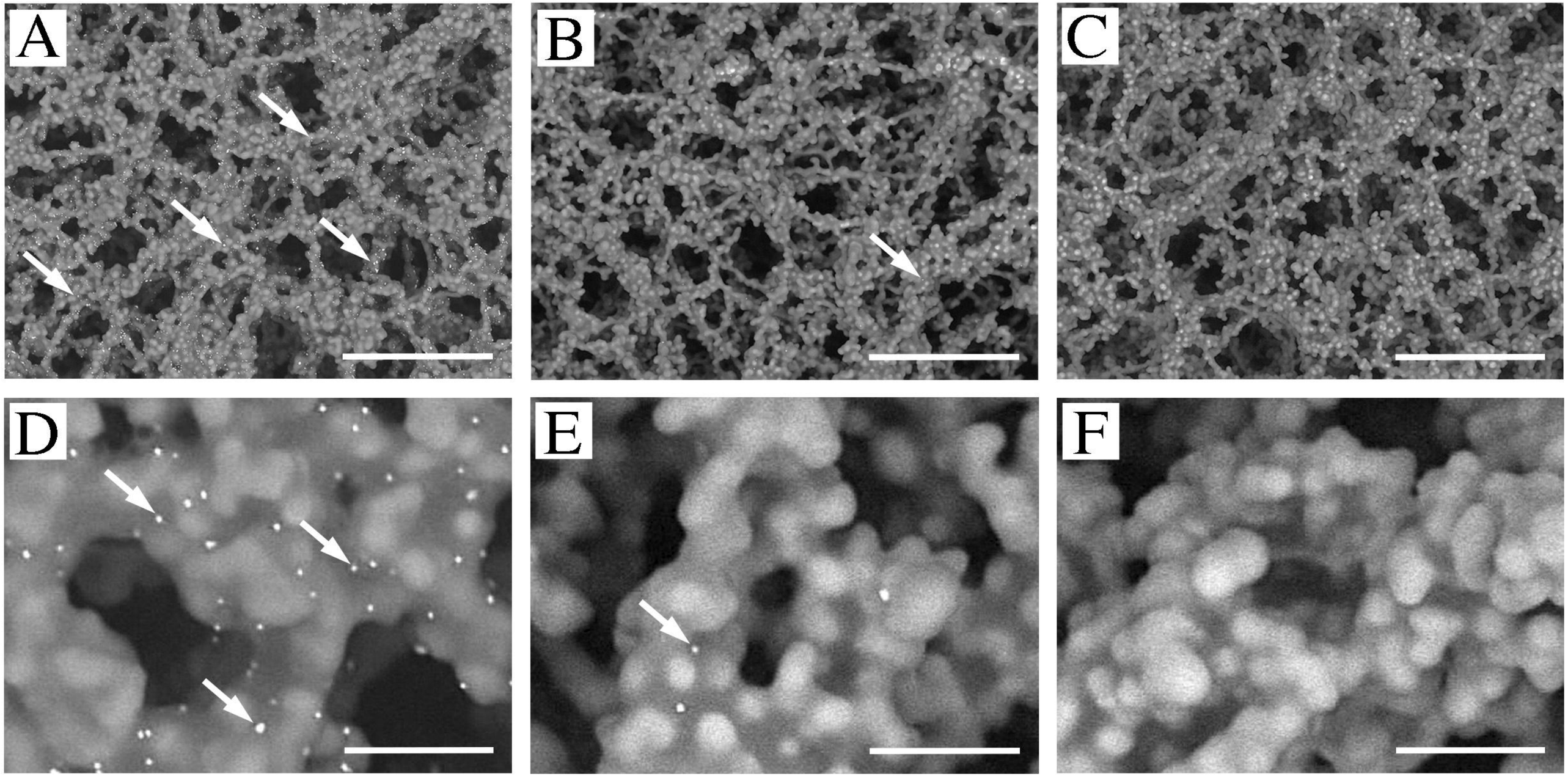
A
B
C
D
E
F

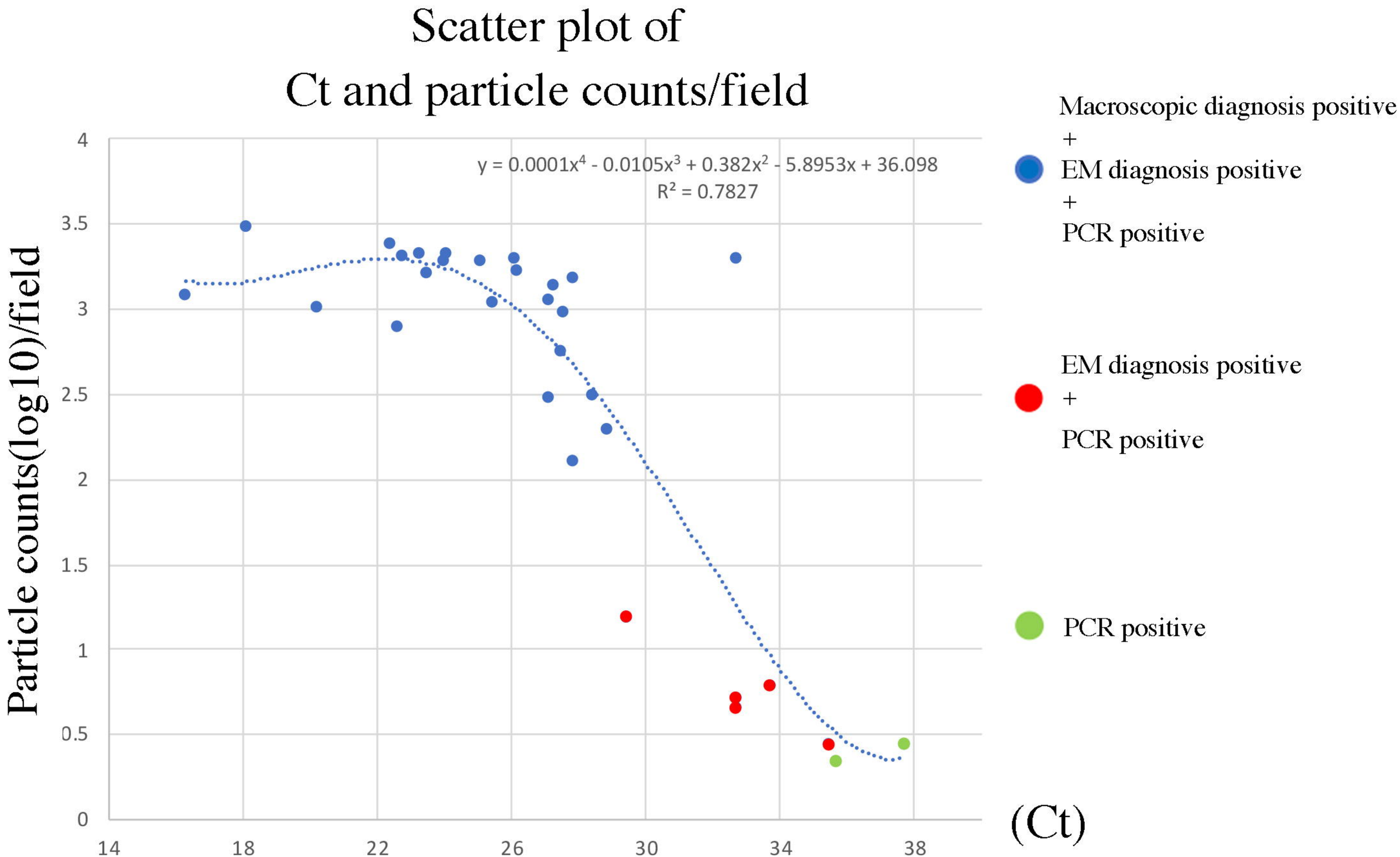
Scatter plot of
Ct and particle counts/field
y = 0.0001x⁴ - 0.0105x³ + 0.382x² - 5.8953x + 36.098
R² = 0.7827
Particle counts(log10)/field
4
3.5
3
2.5
2
1.5
1
0.5
0
14
18
22
26
30
34
38
(Ct)
Macroscopic diagnosis positive
+
EM diagnosis positive
+
PCR positive
EM diagnosis positive
+
PCR positive
PCR positive

Influenza A rRT-PCR	Ct	Macroscopic diagnosis		Electron microscopic diagnosis	
		Sensitivity	Specificity	Sensitivity	Specificity
Positive (n=31)	14.0≤Ct<22.0	100% (3/3)		100% (3/3)	
	22.0≤Ct<30.0	95.2% (20/21)		100% (21/21)	
	30.0≤Ct≤38.0	14.3% (1/7)		71.4% (5/7)	
	14.0≤Ct≤38.0	77.4% (24/31)		93.5% (29/31)	
Negative (n=166)	Ct>38.0		100% (166/166)		100% (166/166)

		Macroscopic diagnosis			Electron microscopic diagnosis		
		positive	negative	Row Marginal	positive	negative	Row Marginal
Influenza A rRT-PCR	Positive	24	7	31	29	2	31
	Negative	0	166	166	0	166	166
Column Marginal		24	172	197	29	168	197
% Agreement(kappa)		0.96: 24+166/197			0.99: 29+166/197		